Transdisciplinary Insights in Life Sciences

ISSN: 2584-2161(Online)
Journal Homepage: www.panainool.com

RESEARCH ARTICLE

Annealing effects on self-assembled structural, morphological properties of ZnO thin films

Arunachalam Arjunan*, & Ananthi Thanga Thamizh Sithan

Department of Physics, Sri Vinayaga College of Arts & Science, Ulundurpet , Tamilnadu, India.

ARTICLE HISTROY

Received 06 December 2023

Revised 08 December 2023

Accepted 18 December 2023

Keywords

Zinc Oxide
Thin films
Spray Pyrolysis
Structural
Optical Properties

ABSTRACT

Zinc Oxide thin films had been deposited on microscopic glass substrate using spray pyrolysis technique at different substrate temperatures. The X-ray diffraction pattern of the prepared films had shown the polycrystalline nature with the preferential orientation along (002) plane. SEM micrograph of the prepared films revealed the uniform distributions of the spherical grains. The presence of zinc and oxygen is confirmed from the peaks at 1 keV, 8 keV and 0.44 keV using EDS analysis. From the optical studies, the high transparency in the visible region with an average transmittance reaching values up to 80% is observed. The calculated values of Energy band gap Eg are found to vary from 3.06 eV to 3.26 eV with increase of substrate temperature from 325°C to 425°C blue, green and red emission.

✉ Arunachalam Arjunan
arunachalamppcu@gmail.com

Introduction

Among various II-VI semiconductor materials, zinc oxide is one of the important semiconducting metal oxide because it has higher electron mobility about 60meV at room temperature, has wide band gap energy of 3.37 eV, n-type conductivity, abundant in nature and environmental friendly. The band gap of the ZnO is similar to the band gap of TiO_2 i.e., 3.2 – 3.3 eV (Firdaus et al., 2012). In addition, ZnO films with high transmittance in the visible region and low resistivity are suitable for use as transparent electrodes in electronic displays. Also it has shown as promising antibacterial agents when it is used for surface coating in food packages and textiles (Cuevas et al., 2013). Thomas et al., (2014) and Voicu et al., (2020) states that apart from other applications of ZnO such as transparent conducting electrode for photovoltaic (solar cells), light emitting diodes, optoelectronic devices, gas sensors etc., it is also used in the pharmaceutics, cosmetics, food science and agriculture. ZnO thin films have been prepared by various techniques such as vapor deposition technique (Mosbah et al., 2005), spray pyrolysis method (Ergin et al., 2009; Vimalkumar et al., 2010), novel chemical deposition technique (Acosta-Osorno et al., 2019; Ali, 2011) Among

these techniques, spray pyrolysis is preferred for deposition of large area coatings. In the present study, we have investigated the effect of molar concentration and deposition temperature on structural, morphological and optical properties of ZnO thin film and it is aimed to deposit ZnO films with preferential orientation along the c-axis.

Material and Methods

ZnO films were deposited at different substrate temperatures (Ts =325, 350, 375, 400 and 425ºC) using spray pyrolysis technique. The precursor of zinc was zincacetylacetonate ($ZnC_{10}H_{14}O_5$) (0.1M) was dissolved in ethanol and sprayed onto microscopic glass substrates with dimensions of 75x25 mm2. Before preparation of films, glass substrates were well cleaned with water bath followed by HCl, acetone and finally rinsed with distilled water and allowed to dry in oven. The substrates were pre-heated for sufficient time before deposition.

Characterization technique

The structural characterization of the deposited films were carried out by X-ray diffraction technique on SHIMADZU-6000 (monochromatic Cu-Kα radiation, λ=1.5406 Å). The surface morphology was studied by using SEM (JEOL-JES-1600). Optical absorption spectrum was recorded in the range of 300-1200 nm using JASCO V-670 spectrophotometer.

Results and Discussion

Structural Studies

Figure 1 shows the XRD patterns of the ZnO thin films prepared at 400°C with different molar concentration. The peak corresponding to (101) plane with low intensity is observed for 0.05M. When the molarity is increased to 0.1M, the peaks corresponding to the planes (002), (101) and (103) are observed. Among these planes, the higher intensity which is observed for the plane (002) shows the preferential orientation along c axis which may be due to the increased Zn incorporation and growth rate (Benramache et al., 2019; Joseph et al., 1999). At 0.15 M, the intensity of (002) plane decreases which may be due to structural disorder or reorientation (Deyu et al., 2019; Khelifi & Attaf, 2020). From the above observation the molarity is fixed as 0.1 M and films are deposited at different substrate temperature with 0.1M to optimize the substrate temperature.

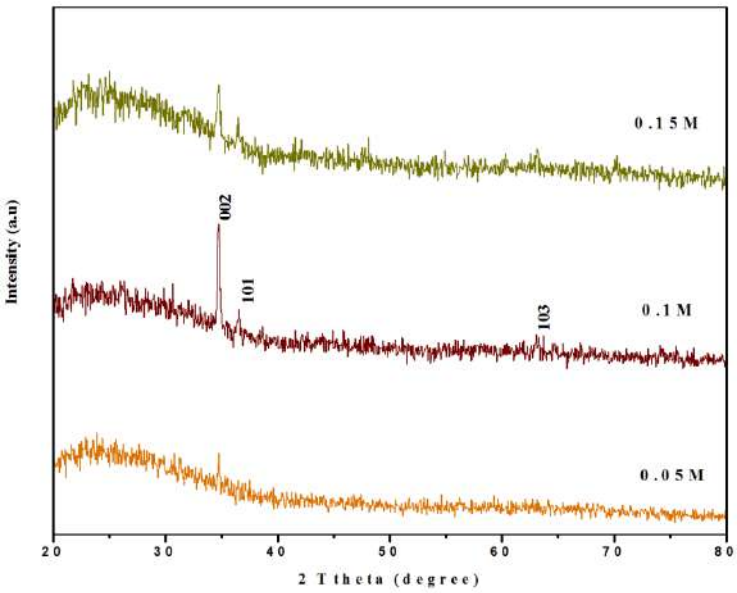

Fig 1. XRD patterns of the ZnO thin films at different molar concentrations.

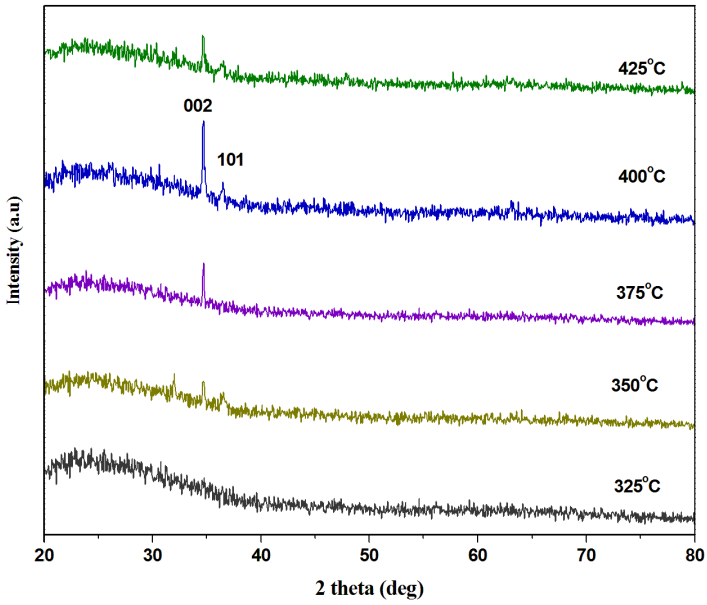

Fig 2. XRD patterns of ZnO thin film deposited at different substrate temperatures.

Table 1. Structural properties of ZnO thin films deposited at different substrate temperatures.

Temperature (˚C)	D (nm)	ε x10^{-3}	δx10^{14} lines/m^2	TC$_{(hkl)}$	Lattice constant (Å)	
					a	c
350	13.96	2.48	51.20	1.16	3.259	5.244
375	30.16	1.13	10.77	1.71	3.249	5.188
400	38.82	0.89	6.63	2.21	3.247	5.198
425	35.77	1.25	7.10	1.41	3.241	5.154

Figure 2 presents the structural information of the films deposited with molar concentration 0.1M at different substrate temperature. The absence of zinc oxide peaks such as (100), (101) and (002) at substrate temperature 325˚C is due to insufficient temperature for the reaction to produce zinc oxide with better crystallinity. The film deposited at the substrate temperature 350˚C are polycrystalline with peaks at (31.05°), (34.65°) and (36.50°) corresponding to (100), (002) and (101) planes respectively. As the substrate temperature increases to 375˚C, the peaks of (100) and (101) nearly disappear and the single peak of (002) with low intensity (Kim et al., 2005; Siregar & Motlan, 2018). The film deposited at 400°C is polycrystalline and oriented along (002) plane being predominant and belongs to hexagonal wurtzite structure and (101) and (103) planes are observed with low intensity, indicating the better crystallinity. The intensity of (100) and (103) planes become very low may be due to the diffusion of atoms which are absorbed on the substrate. The increased substrate temperature 400°C is in favour to the diffusion of atoms absorbed on the surface to the energy favorable positions, and thus the film is oriented along c-axis, which is indicated by the increased intensity of (002) reflections (Singh et al., 2007). At 425°C, there is a significant decomposition of aerosol droplets on the preheated substrate, which lead to the decrease in intensity of the peak correspond to (002) plane (Mosbah et al., 2005).

The diffraction peaks presented in the data are indexed with the JCPDS data (card no. 36-1451). The obtained unit cell parameters a = 3.253Å and c = 5.123Å are almost equal to the standard a = 3.385Å and c = 5.076Å. The preheating and substrate temperature plays vital role in the growth of ZnO thin films with preferential orientation along (002) plane (c-axis orientation). The crystallite size ($\boldsymbol{D = \frac{\kappa\lambda}{\beta cos\theta}}$ **x 10^{-9} m**), strain $\boldsymbol{\varepsilon = \frac{\beta cos\theta}{4}}$, and dislocation density ($\boldsymbol{\delta = \frac{1}{D^2}}$ lines/m2) are calculated using the formula that is reported by Arunachalam et al., (2016). From the Table 1, it is observed that the crystallite size increases with the decrease of strain and dislocation density which indicate the better crystallinity (Zahedi et al., 2014), whereas at higher substrate temperature (425°C), the crystallite size decreases with increase of strain and dislocation density which indicates the deterioration of the film. As from the Table 1, the strain and the stress decreases with increase in the grain size shows that the atoms receive sufficient energy for the improvement of the rearrangement of the atoms which is resulting in the reduction of crystal defects (stress/strain) in the film. Therefore, it is clearly noted that the compressive stresses are closely related to the structural modification (Rao et al., 2009). The texture coefficient (TC) represents the texture of particular plane, deviation of which from unity implies the preferred growth. Quantitative information concerning the preferential crystallite orientation was obtained from the different texture coefficient TC$_{(hkl)}$ defined as

$$TC_{(hkl)} = \frac{\frac{I_{(hkl)}}{I_{0(hkl)}}}{1/n \sum \frac{I_{hkl}}{I_{0(hkl)}}},$$

Where $TC_{(hkl)}$ is the texture coefficient, $I_{(hkl)}$ is the XRD intensity and n is number of diffraction peaks considered. $I0_{(hkl)}$ is the intensity of the XRD reference of the randomly oriented grains. The texture coefficient ($TC_{(hkl)}$) represents the texture of particular plane, deviation of which from unity implies the preferred growth. The higher texture coefficient values ($TC_{(hkl)}$ >1) with increasing substrate temperature states the abundance of the grains in the (hkl) direction (Table1). The value of the texture coefficient is maximum at 400°C, the preferential growth of the crystallites is increased and is perpendicular to the (hkl) plane. The highest $TC_{(hkl)}$ value of 2.21 is observed for the plane (002). Hence substrate temperature of 400°C is optimized temperature for the growth of c-axis oriented films. The decrease of $TC_{(hkl)}$ value of (002) plane for the film deposited at 425°C is with the randomly oriented crystallites (Amakali et al., 2020) . It has been observed that lattice constant decreases with increase of grain size. The difference in lattice parameters may be due to the change in the nature and concentration of the native imperfections which may cause the elongation or compression of lattice parameters (Kumar & Reddy, 2013; Senthilkumar et al., 2010).

SEM Studies and Compositional analysis

Fig. 3 shows the SEM micrographs of the films deposited at different substrate temperatures. The average grain size of 200 nm, 250 nm, 450 nm and 800 nm is observed for the films deposited with substrate temperature 350, 375, 400 and 425°C respectively, similar range of grain size is observed by Mani & Rayappan, (2013) for ZnO films using spray technique. SEM image of (Fig 2a) shows the distribution of grains in a random manner. At 375°C (Fig 3b), though the grains are visible, they are smaller in size with compact nature. The development of smooth, dense and uniform grains with good adhesion to the substrate is observed with the increasing substrate temperature (400°C) (Fig 3c). A further increase in grain size is observed for the film deposited at substrate temperature 425°C (Fig 3d).

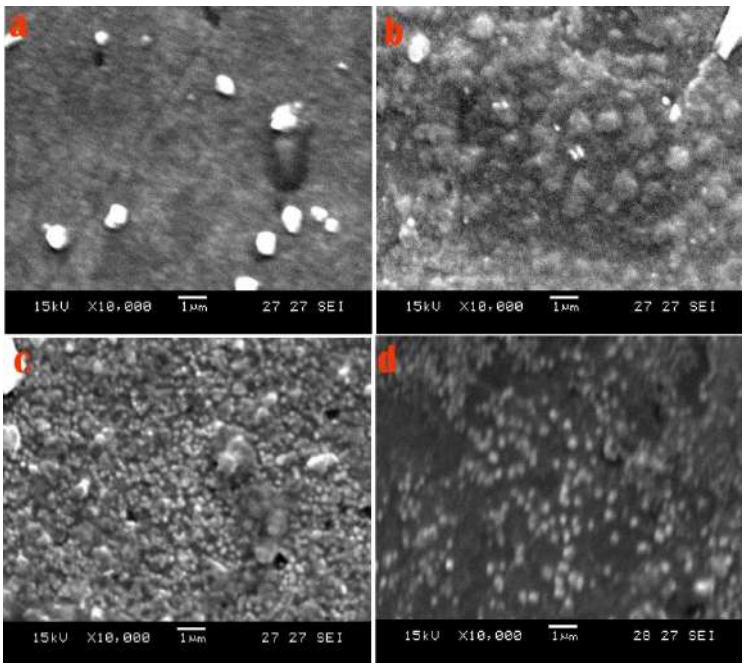

Fig 3. SEM images of ZnO thin films grown at substrate temperature of a) 325°C, b) 375°C, c) 400°C, d) 425°C of the films

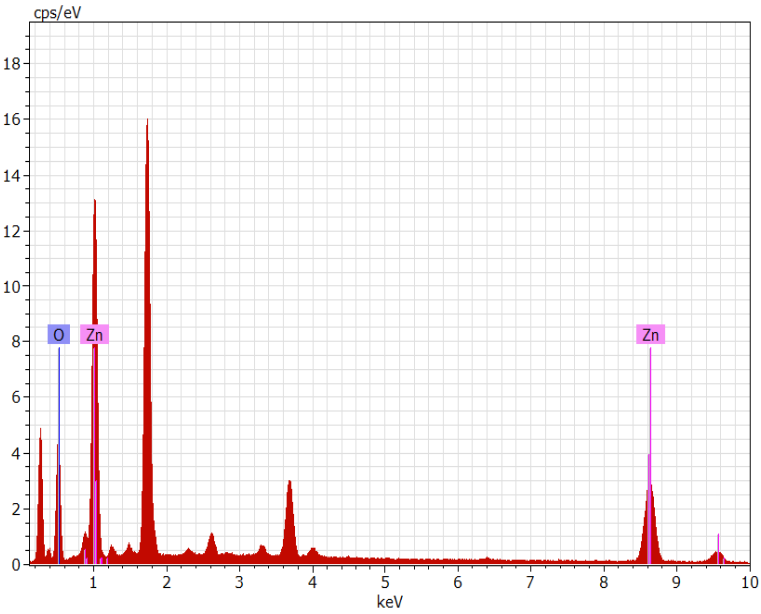

Fig 4. EDS spectrum of ZnO thin filmat 400°C

The elemental composition of the films examined by EDS analysis is shown in the Fig 4. The presence of zinc and oxygen is confirmed from the peaks at 1 keV, 8 keV and 0.44 keV respectively. The presences of other peaks are due to the glass substrate. The relativity near stiochiometry is revealed from the presence of elements Zn and O with atomic percentage 42.49 and 57.51 respectively.

Optical studies

Transmittance

The optical transmission spectra recorded in the wavelength range of 350-1200 nm is shown in the Fig.5. The transmission is increased from 68-80% with the increase of deposition temperature from 325-425°C. The transmission spectra of the films show high transparency in the visible region with an average transmittance reaching values up to 80% indicate better crystal structure with less defects obtained at higher substrate temperature. A sharp ultraviolet cut-off at approximately 380 nm is observed for all the films (Tarwal et al., 2011). Liu et al., (2012) have stated that films with higher transparency in the visible region can act as a transparent conducting oxide material in the photovoltaic cell applications. The high transparency obtained for the film in the visible region shows its potential application in the photovoltaic device applications.

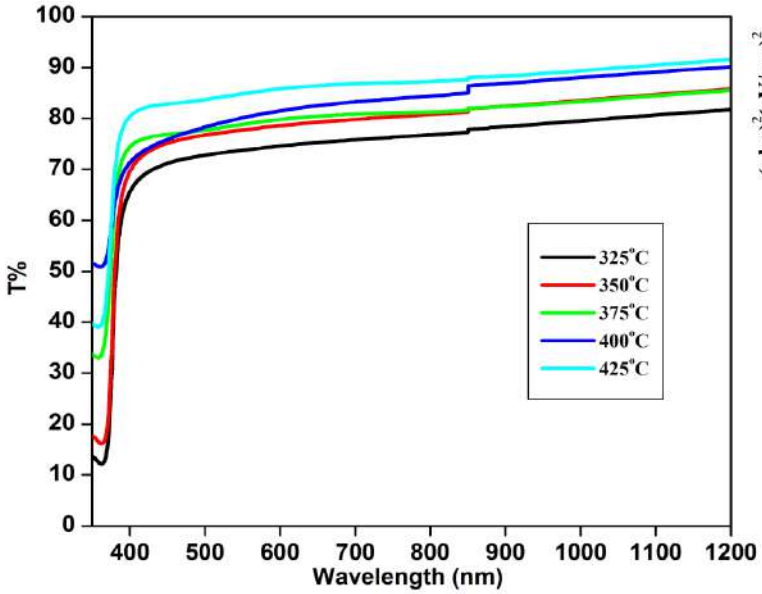

Fig 5. UV-Vis Transmission spectra of ZnO thin films

Band gap

The optical band gap of the ZnO films is estimated from the relation

$$(\alpha h\nu)^2 = A(h\nu - E_g)$$

where E_g is the optical band gap and A is a constant. Fig 6 shows the optical direct band gap of ZnO thin films. The calculated values of band gap Eg are found to vary from 3.06 eV to 3.26eV with increase of substrate temperature from 325°C to 425°C. It is observed that the band gap is increased with increase in grain size. The variation of band gap of thin films is generally due to individual or combined effect of some factors like band filling effect, quantum size confinement causing increase in band gap with increase of grain size, charged impurities at the grain boundaries, lattice strain present in the films and the extent of structural disorder. As the substrate temperature increases there is a decrease in the structural disorder in the films which is probably due to the reduction of defects at the grain boundaries of the layers leading to an increase in the value of band gap.

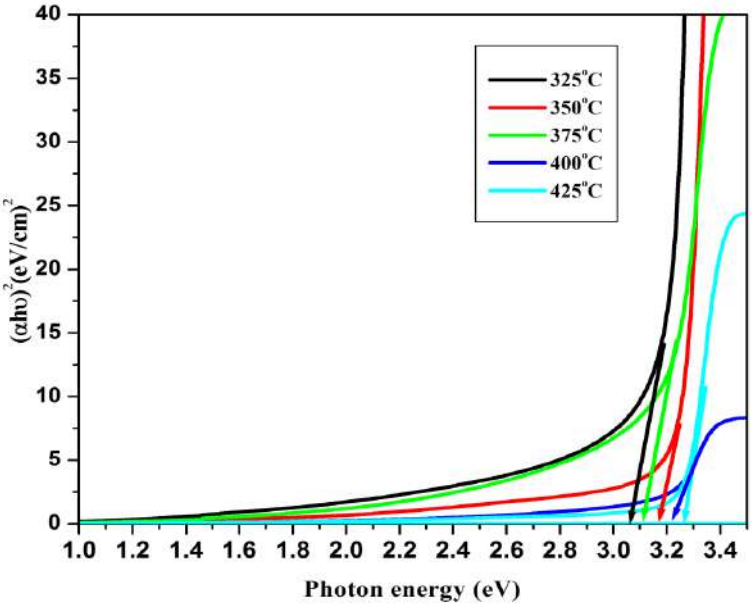

Fig 6. Plot of (αhν)1/2 versus photon energy

Photoluminescence studies

The PL spectrum of the ZnO film (Fig 7) deposited at 400°C, the peak at 418 nm is the violet emission which is attributed to the free excitonic emission of radiative defects. Similar result is also obtained by (Kumar & Reddy, 2013) and the author has stated that the violet peak is attributed to free excitonic emission because of the high binding energy of 60 meV. The observed blue emission of 441 nm is originated from exciton recombination between the electrons localised at the zinc interstitials and the holes in the valence band. As the substrate

temperature increased a small hump is observed at 671 nm, which may be due to the native defects such as Zn interstitials or oxygen vacancies. The suppression of the green emission at around 525 nm may be due to the presence of minimum crystal defects in the film. The PL emission characteristics of ZnO films are strongly dependent on both the crystal quality and the stoichiometry of the film (Tarwal et al., 2011).

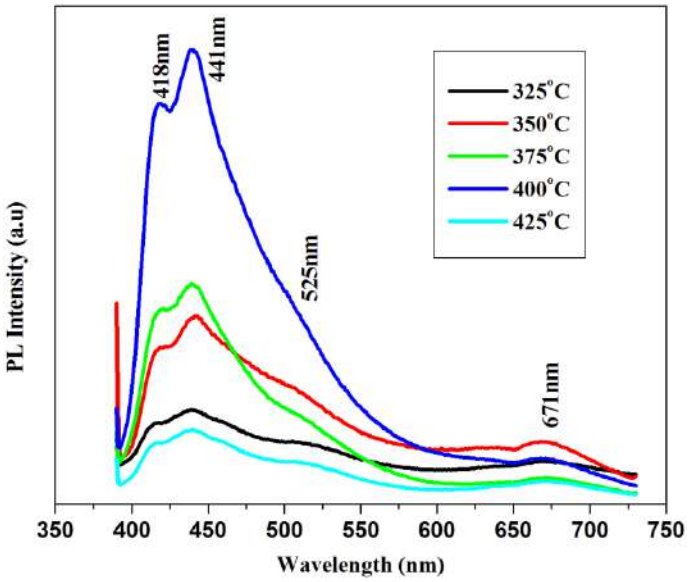

Fig 7. Photoluminescence spectra of the ZnO thin film

Conclusion

XRD pattern of ZnO thin films prepared by spray pyrolysis method revealed the hexagonal wurtzite structure with preferential orientation along c-axis, which is suitable for dye-sensitized solar cell (DSSC) applications. It is observed that the films prepared with 0.1 M are well crystallized and is preferentially orientated along (002) plane.

ZnO thin films are deposited on glass substrate at substrate temperature from 325 - 475°C with 0.1M. From the XRD patterns, the film deposited with the substrate temperature 400°C shows the orientation along (002) plane with the maximum crystallite size of 38.82 nm. The development of smooth, dense and uniform grains with good adhesion to the substrate is observed in SEM analysis for the film deposited at the substrate temperature 400°C. The films are highly transparent in the visible region with an average transmittance reaching upto 80%, which indicates the better crystalline nature with less defects. The calculated values of band gap are found to be increased upto 3.22 eV. PL spectra of the films have shown emission in the visible region at 418 nm, 441 nm, 525 nm and 671 nm. The minimum resistivity is observed for the film deposited at 400°C. Therefore, the film deposited with molarity 0.1M and the substrate temperature of 400°C shows the better results and considered to be as optimized parameters.

Acknowledgments

The authors are grateful to the Department of Physics, Sri Vinayga college of Arts & Sicence, Ulundurpet, Tamil Nadu, India and also thankful to Annamalai Univeristy for providing laboratory facilities.

Conflict of interest

All authors declare that there is no conflict of interest in this work.

References

Acosta-Osorno, M., Alcántara-Iniesta, S., Alvarado, J., Young, C. D., Mejía, I., García, M., Ramos-Serrano, J. R., & Juarez-Díaz, G. (2019). Characterization of ZnO thin films obtained by ultrasonic spray pyrolysis for application in UV photoconductive detectors. *Materials Research Express*, *6*(11), 116450. https://doi.org/10.1088/2053-1591/ab4fc3

Ali, M. M. (2011). *Characterization of ZnO thin films grown by chemical bath deposition*. *37*(3).

Amakali, T., Daniel, L. S., Uahengo, V., Dzade, N. Y., & de Leeuw, N. H. (2020). Structural and Optical Properties of ZnO Thin Films Prepared by Molecular Precursor and Sol–Gel Methods. *Crystals*, *10*(2). https://doi.org/10.3390/cryst10020132

Arunachalam, A., Dhanapandian, S., & Manoharan, C. (2016). Effect of Sn doping

on the structural, optical and electrical properties of TiO2 films prepared by spray pyrolysis. *Physica E: Low-Dimensional Systems and Nanostructures*, *76*, 35–46. https://doi.org/https://doi.org/10.1016/j.physe.2015.09.048

Benramache, S., Aoun, Y., Lakel, S., & Benhaoua, B. (2019). The effect of film thickness on the structural, optical and electrical properties of ZnO thin films deposited by ultrasonic spray deposition. *Materials Research Express*, *6*(12), 126418. https://doi.org/10.1088/2053-1591/ab574a

Cuevas, A. G., Balangcod, K., Balangcod, T., & Jasmin, A. (2013). Surface Morphology, Optical Properties and Antibacterial Activity of Zinc Oxide Films Synthesized via Spray Pyrolysis. *Procedia Engineering*, *68*, 537–543. https://doi.org/https://doi.org/10.1016/j.proeng.2013.12.218

Deyu, G. K., Muñoz-Rojas, D., Rapenne, L., Deschanvres, J.-L., Klein, A., Jiménez, C., & Bellet, D. (2019). SnO2 Films Deposited by Ultrasonic Spray Pyrolysis: Influence of Al Incorporation on the Properties. *Molecules*, *24*(15). https://doi.org/10.3390/molecules24152797

Ergin, B., Ketenci, E., & Atay, F. (2009). Characterization of ZnO films obtained by ultrasonic spray pyrolysis technique. *International Journal of Hydrogen Energy*, *34*(12), 5249–5254. https://doi.org/https://doi.org/10.1016/j.ijhydene.2008.09.108

Firdaus, C. M., Rizam, M. S. B. S., Rusop, M., & Hidayah, S. R. (2012). Characterization of ZnO and ZnO: TiO2 Thin Films Prepared by Sol-Gel Spray-Spin Coating Technique. *Procedia Engineering*, *41*, 1367–1373. https://doi.org/https://doi.org/10.1016/j.proeng.2012.07.323

Joseph, B., Gopchandran, K. G., Thomas, P. V, Koshy, P., & Vaidyan, V. K. (1999). A study on the chemical spray deposition of zinc oxide thin films and their structural and electrical properties. *Materials Chemistry and Physics*, *58*(1), 71–77. https://doi.org/https://doi.org/10.1016/S0254-0584(98)00257-0

Khelifi, C., & Attaf, A. (2020). Influence of Ti doping on SnO2 thin films properties prepared by ultrasonic spray technique. *Surfaces and Interfaces*, *18*, 100449. https://doi.org/https://doi.org/10.1016/j.surfin.2020.100449

Kim, Y.-S., Tai, W.-P., & Shu, S.-J. (2005). Effect of preheating temperature on structural and optical properties of ZnO thin films by sol–gel process. *Thin Solid Films*, *491*(1), 153–160. https://doi.org/https://doi.org/10.1016/j.tsf.2005.06.013

Kumar, G. A., & Reddy, K. N. (2013). *Structural, Optical and Electrical Characteristics of Nanostructured ZnO Thin Films with various Thicknesses deposited by RF Magnetron Sputtering*. https://api.semanticscholar.org/CorpusID:55872605

Liu, J., Ma, S. Y., Huang, X. L., Ma, L. G., Li, F. M., Yang, F. C., Zhao, Q., & Zhang, X. L. (2012). Effects of Ti-doped concentration on the microstructures and optical properties of ZnO thin films. *Superlattices and Microstructures*, *52*(4), 765–773. https://doi.org/https://doi.org/10.1016/j.spmi.2012.06.021

Mani, G. K., & Rayappan, J. B. B. (2013). A highly selective room temperature ammonia sensor using spray deposited zinc oxide thin film. *Sensors and Actuators B: Chemical*, *183*, 459–466. https://doi.org/https://doi.org/10.1016/j.snb.2013.03.132

Mosbah, A., Moustaghfir, A., Abed, S., Bouhssira, N., Aida, M. S., Tomasella, E., & Jacquet, M. (2005). Comparison of the structural and optical properties of zinc oxide thin films deposited by d.c. and r.f. sputtering and spray pyrolysis. *Surface and Coatings Technology*, *200*(1), 293–296.

https://doi.org/https://doi.org/10.1016/j.surfcoat.2005.02.012

Rao, T. P., Kumar, M. C. S., Angayarkanni, S. A., & Ashok, M. (2009). Effect of stress on optical band gap of ZnO thin films with substrate temperature by spray pyrolysis. *Journal of Alloys and Compounds*, *485*(1), 413–417. https://doi.org/https://doi.org/10.1016/j.jallcom.2009.05.116

Senthilkumar, K., Tokunaga, M., Okamoto, H., Senthilkumar, O., Lin, J., Urban, B., Neogi, A., & Fujita, Y. (2010). Multiphonon scattering and non-radiative decay in ZnO nanoparticles. *Physica Status Solidi (C) Current Topics in Solid State Physics*, *7*(6), 1586–1588. https://doi.org/10.1002/pssc.200983203

Singh, P., Kumar, A., Deepak, & Kaur, D. (2007). Growth and characterization of ZnO nanocrystalline thin films and nanopowder via low-cost ultrasonic spray pyrolysis. *Journal of Crystal Growth*, *306*(2), 303–310. https://doi.org/https://doi.org/10.1016/j.jcrysgro.2007.05.023

Siregar, N., & Motlan. (2018). The Effect of Pre-heating Temperature on Structural and Optical Properties ZnO Thin Film Synthesized using Sol-Gel spin Coating Method. *Journal of Physics: Conference Series*, *1120*(1), 12088. https://doi.org/10.1088/1742-6596/1120/1/012088

Tarwal, N. L., Shinde, V. V, Kamble, A. S., Jadhav, P. R., Patil, D. S., Patil, V. B., & Patil, P. S. (2011). Photoluminescence and photoelectrochemical properties of nanocrystalline ZnO thin films synthesized by spray pyrolysis technique. *Applied Surface Science*, *257*(24), 10789–10794. https://doi.org/https://doi.org/10.1016/j.apsusc.2011.07.099

Thomas, D., Abraham, J., Vattappalam, S. C., Augustine, S., & DennisThomas, T. (2014). Antibacterial activity of pure and cadmium doped zno thin film. *Indo American Journal of Pharmaceutical Research*, *4*, 1612–1616. https://api.semanticscholar.org/CorpusID:93173475

Vimalkumar, T. V, Poornima, N., Kartha, C. S., & Vijayakumar, K. P. (2010). Effect of precursor medium on structural, electrical and optical properties of sprayed polycrystalline ZnO thin films. *Materials Science and Engineering: B*, *175*(1), 29–35. https://doi.org/https://doi.org/10.1016/j.mseb.2010.06.012

Voicu, G., Miu, D., Ghitulica, C.-D., Jinga, S.-I., Nicoara, A.-I., Busuioc, C., & Holban, A.-M. (2020). Co doped ZnO thin films deposited by spin coating as antibacterial coating for metallic implants. *Ceramics International*, *46*(3), 3904–3911. https://doi.org/https://doi.org/10.1016/j.ceramint.2019.10.118

Zahedi, F., Dariani, R. S., & Rozati, S. M. (2014). Structural, Optical and Electrical Properties of ZnO Thin Films Prepared by Spray Pyrolysis: Effect of Precursor Concentration. *Bulletin of Materials Science*, *37*(3), 433–439. https://doi.org/10.1007/s12034-014-0696-8